

Shift-invariant spaces, bandlimited spaces and reproducing kernel spaces with shift-invariant kernels on undirected finite graphs

Seok-Young Chung and Qiyu Sun

Abstract

In this paper, we introduce the concept of graph shift-invariant space (GSIS) on an undirected finite graph, which is the linear space of graph signals being invariant under graph shifts, and we study its bandlimiting, kernel reproducing and sampling properties.

Graph bandlimited spaces have been widely applied where large datasets on networks need to be handled efficiently. In this paper, we show that every GSIS is a bandlimited space, and every bandlimited space is a principal GSIS.

Functions in a reproducing kernel Hilbert space with shift-invariant kernel could be learnt with significantly low computational cost. In this paper, we demonstrate that every GSIS is a reproducing kernel Hilbert space with a shift-invariant kernel.

Based on the nested Krylov structure of GSISs in the spatial domain, we propose a novel sampling and reconstruction algorithm with finite steps, with its performance tested for well-localized signals on circulant graphs and flight delay dataset of the 50 busiest airports in the USA.

I. INTRODUCTION

A shift-invariant space (SIS) H of functions on the line is a linear space invariant under integer shifts, i.e., $f(\cdot - k) \in H$ for all $f \in H$ and $k \in \mathbb{Z}$. It has been widely used in approximation theory, wavelet analysis, sampling theory, Gabor analysis and many other mathematical and engineering fields [1], [2], [3], [4], [5], [6], [7]. Bandlimited spaces and principal shift-invariant spaces are two typical examples of SISs.

Graph signal processing offers a unique opportunity to represent, process, analyze, and visualize graph signals and network data [8], [9], [10], [11], [12], [13]. Similar to the one-order delay in classical signal processing, the concept of graph shifts has been introduced in graph signal processing. Graph shifts are usually selected to have specific features, and designed to capture the topology of the underlying graph. Their illustrative examples include the adjacency and Laplacian matrices of the underlying graph and their variants. In this paper, we introduce the concept of graph shift-invariant space (GSIS) on an undirected finite graph, which is the linear space of graph signals being invariant under graph shifts; see (III.1), and we study various properties of GSISs on bandlimiting, kernel reproducing and sampling.

Based on graph Fourier transform on undirected graphs, bandlimited spaces of graph signals have been well-defined; see (III.3) and [14], [15], [16], [17], [18], [19]. One may verify that every graph bandlimited space is invariant under graph shifts. The first main contribution of this paper is to demonstrate that every GSIS is a bandlimited space and every bandlimited space is a principal graph shift-invariant space (PGSIS); see Theorems III.1 and III.2. Therefore the terminologies on bandlimitedness, shift-invariance and principal-shift-invariance of a linear space of graph signals are essentially the same in the undirected finite graph setting, with the first one illustrating its bandlimiting property in the Fourier domain, the second one emphasizing its shift-invariance in the spatial domain, and the third one highlighting the spatial-frequency localization for its generator.

Reproducing kernel Hilbert spaces (RKHSs) on the line have been widely accepted in kernel-based learning for function estimation [20], [21], [22], [23], [24]. For efficient learning of functions in a RKHS on an undirected graph, the kernel are usually selected to be shift-invariant; see (IV.1). RKHSs with shift-invariant kernels (SIGRKHSs) have the inner product being defined by a generalized dot product in the Fourier domain; see Theorem IV.2, and

shift-invariant kernels could be learnt with significantly low computational cost. Common selection of such shift-invariant kernels includes diffusion kernels, regularization kernels, random walk kernels and spline kernels [25], [26], [27], [28], [29], [30], [31], [32], [33], [34], [35]. A SIGRKHS is clearly invariant under graph shifts. The second main contribution of this paper is to show that the converse is also true; see Theorem IV.1.

SISs and RKHSs on the line are suitable for modeling time signals with smoother spectrum, and for sampling and numerical implementation of signal reconstruction [3], [5], [6], [7], [36]. Flight delays cause a ripple effect throughout the entire airport network. Our numerical simulations indicate that the on-time performance data of the 50 busiest airports in the USA can be modelled as graph signals living more suitable in a GSIS with the generators appropriately chosen than in a bandlimited space; see Section VI-B. We observe that every PGSIS (hence graph bandlimited space and graph shift-invariant space in general) has the nested Krylov structure; see (V.8). The third main contribution of this paper is to establish a sampling theorem for a PGSIS and propose an iterative algorithm with finite steps for graph signal reconstruction, see Theorem V.1, Corollaries V.2 and V.3, and Algorithm V.1. Our numerical simulations in Section VI show that the proposed Algorithm V.1 has good performance to reconstruct well-localized signals in a GSIS on circulant graphs and the flight delay dataset of the 50 busiest airports in the USA.

The paper is organized as follows. In order to define GSISs, bandlimited spaces and SIGRKHSs on undirected graphs, in Section II we recall some preliminaries on graph shifts, polynomial filters, and graph Fourier transform. In Section III, we introduce GSISs, graph bandlimited spaces and GSISs generated by a family of graph signals, and show that they are essentially the same; see Theorem III.1. In Section III, we also provide an estimate to Riesz/frame bounds for shifts of the generator of a PGSIS; see Propositions III.3 and III.4, and based on the graph uncertainty principle, we show that a PGSIS generated by a localized graph signal has large dimension; see Proposition III.5. In Section IV, we introduce the concept of shift-invariant kernel, discuss the inner product structure of SIGRKHSs, and show that every GSIS embedded with standard Euclidean inner product is a SIGRKHS; see (IV.1), and Theorems IV.1 and IV.2. In Section V, we consider sampling and reconstruction of signals in a PGSIS; see Theorem V.1, Corollary V.2 and Algorithm V.1. Performance of Algorithm V.1 for signal reconstruction is presented in Section VI. All proofs are collected in Section VII.

Notation: We denote its standard inner product and p -norm on the Euclidean space \mathbb{R}^N by $\langle \cdot, \cdot \rangle$ and $\| \cdot \|_p, 1 \leq p \leq \infty$, respectively. We use $\langle \cdot, \cdot \rangle_H$ and $\| \cdot \|_H$ to represent the inner product and norm on a Hilbert space H . For a matrix \mathbf{A} , we denote its transpose, maximal singular value, minimal singular value and minimal nonzero singular value by $\mathbf{A}^T, \sigma_{\max}(\mathbf{A}), \sigma_{\min}(\mathbf{A})$ and $\sigma_{\min}^+(\mathbf{A})$ respectively. As usual, we denote the set of nonnegative integers by \mathbb{Z}_+ , the cardinality of a set W by $\#W$, the support of a vector $\mathbf{x} \in \mathbb{R}^N$ by $\text{supp } \mathbf{x}$ and the dimension of a linear space H by $\dim H$. Also we set $\mathbb{Z}_+^L = \{[\alpha_1, \dots, \alpha_L] \mid \alpha_1, \dots, \alpha_L \in \mathbb{Z}_+\}, L \geq 1$ and define $|\boldsymbol{\alpha}| = \alpha_1 + \dots + \alpha_L$ for $\boldsymbol{\alpha} = [\alpha_1, \dots, \alpha_L] \in \mathbb{Z}_+^L$.

II. PRELIMINARIES ON GRAPH SHIFTS AND GRAPH FOURIER TRANSFORM

Polynomial filters have been widely used in graph signal processing, and graph shifts are building blocks for polynomial filters [8], [9], [13], [34], [37], [38], [39]. In this section, we first recall some preliminaries on graph shifts and polynomial filters.

Graph Fourier transform (GFT) decomposes graph signals into different frequency components, and it provides a powerful way to analyze and process graph signals. Based on multiple commutative graph shifts, in this section we then define GFT on undirected graphs [8], [10], [12], [13], [24], [40], [41].

A. Graph shifts

Let $\mathcal{G} = (V, E)$ be an undirected graph of order $N \geq 1$. We say that $\mathbf{S} = [S(i, j)]_{i, j \in V}$ is a *graph shift* if $S(i, j) = 0$ except that either $i = j$ or $(i, j) \in E$. Illustrative examples of graph shifts are the adjacency matrix \mathbf{A} , the Laplacian matrix $\mathbf{L} = \mathbf{D} - \mathbf{A}$, the symmetric normalized Laplacian matrix $\mathbf{L}^{\text{sym}} := \mathbf{D}^{-1/2} \mathbf{L} \mathbf{D}^{-1/2}$, and their variants, where \mathbf{D} is the degree matrix. Similar to the one-order delay in classical multidimensional signal processing, the concept of multiple commutative graph shifts $\mathbf{S}_1, \dots, \mathbf{S}_L$ is introduced in [34]. Here graph shifts $\mathbf{S}_1, \dots, \mathbf{S}_L$ are said to be *commutative* if

$$\mathbf{S}_l \mathbf{S}_{l'} = \mathbf{S}_{l'} \mathbf{S}_l, \quad 1 \leq l, l' \leq L. \quad (\text{II.1})$$

Under additional real-valued and symmetric assumptions, they can be diagonalized simultaneously by some orthogonal matrix \mathbf{U} , i.e.,

$$\mathbf{S}_l = \mathbf{U}\mathbf{\Lambda}_l\mathbf{U}^T, \quad 1 \leq l \leq L, \quad (\text{II.2})$$

for some diagonal matrices $\mathbf{\Lambda}_l = \text{diag} [\lambda_l(n)]_{1 \leq n \leq N}, 1 \leq l \leq L$ [24], [34]. With the help of the simultaneous diagonalization (II.2), we define *joint spectrum* of commutative graph shifts $\mathbf{S}_1, \dots, \mathbf{S}_L$ by

$$\mathbf{\Lambda} = \{ \boldsymbol{\lambda}(n) = [\lambda_1(n), \dots, \lambda_L(n)]^T \mid 1 \leq n \leq N \} \subset \mathbb{R}^L. \quad (\text{II.3})$$

In this paper, we make the following assumption on the graph shifts $\mathbf{S}_1, \dots, \mathbf{S}_L$ and their joint spectrum $\mathbf{\Lambda}$.

Assumption II.1. *Graph shifts $\mathbf{S}_1, \dots, \mathbf{S}_L$ are real-valued, symmetric and commutative, and elements $\boldsymbol{\lambda}(n), 1 \leq n \leq N$, of the joint spectrum $\mathbf{\Lambda}$ in (II.3) are distinct.*

B. Polynomial filters

We say that a filter \mathbf{H} is a *polynomial filter* of graph shifts $\mathbf{S}_1, \dots, \mathbf{S}_L$ if there exists a multivariate polynomial $h(t_1, \dots, t_L) = \sum_{[\alpha_1, \dots, \alpha_L] \in \mathbb{Z}_+^L} h_{\alpha_1, \dots, \alpha_L} t_1^{\alpha_1} \dots t_L^{\alpha_L}$ such that

$$\mathbf{H} = h(\mathbf{S}_1, \dots, \mathbf{S}_L) = \sum_{[\alpha_1, \dots, \alpha_L] \in \mathbb{Z}_+^L} h_{\alpha_1, \dots, \alpha_L} \mathbf{S}_1^{\alpha_1} \dots \mathbf{S}_L^{\alpha_L}, \quad (\text{II.4})$$

where the sum is taken on a finite subset of \mathbb{Z}_+^L . A significant advantage is that the filtering procedure associated with a polynomial filter can be implemented at the vertex level in which each vertex is equipped with a one-hop communication subsystem [34]. For a polynomial filter \mathbf{H} , one may verify that it *commutes* with graph shifts $\mathbf{S}_1, \dots, \mathbf{S}_L$, i.e., $\mathbf{H}\mathbf{S}_l = \mathbf{S}_l\mathbf{H}, 1 \leq l \leq L$. The converse is shown to be true in [37] for $L = 1$ and [34, Theorem A.3] for $L \geq 1$.

Proposition II.2. *Let \mathcal{G} be a undirected finite graph, and $\mathbf{S}_1, \dots, \mathbf{S}_L$ be graph shifts satisfying Assumption II.1. Then \mathbf{H} commutes with graph shifts $\mathbf{S}_1, \dots, \mathbf{S}_L$ if and only if it is a polynomial filter.*

By (II.2) and Proposition II.2, we see that a filter commuting with commutative graph shifts is diagonalizable.

Corollary II.3. *Let \mathbf{U} be the orthogonal matrix in (II.2) and \mathbf{H} be a filter commuting with graph shifts $\mathbf{S}_1, \dots, \mathbf{S}_L$. Then $\mathbf{U}\mathbf{H}\mathbf{U}^T$ is a diagonal matrix.*

C. Graph Fourier transform

For the orthogonal matrix \mathbf{U} in (II.2), we write $\mathbf{U} = [\mathbf{u}_1, \dots, \mathbf{u}_N]$. Under Assumption II.1, the orthogonal matrix to diagonalize graph shifts $\mathbf{S}_1, \dots, \mathbf{S}_L$ simultaneously is **unique** up to some sign change, in the sense that, for any orthogonal matrix $\mathbf{V} = [\mathbf{v}_1, \dots, \mathbf{v}_N]^T$ satisfying $\mathbf{S}_l = \mathbf{V}\mathbf{\Lambda}_l\mathbf{V}^T, 1 \leq l \leq L$, there exists a diagonal matrix $\mathbf{P} = \text{diag}[\epsilon_1, \dots, \epsilon_n]$ for some $\epsilon_n \in \{-1, 1\}, 1 \leq n \leq N$, such that $\mathbf{V} = \mathbf{U}\mathbf{P}$, or equivalently, $\mathbf{v}_n = \epsilon_n \mathbf{u}_n$ for all $1 \leq n \leq N$. In particular, one may verify that $\mathbf{P} := \mathbf{U}^T \mathbf{V}$ satisfies $\mathbf{P}\mathbf{\Lambda}_l = \mathbf{\Lambda}_l \mathbf{P}$ for all $1 \leq l \leq L$, by the simultaneous diagonalization property for graph shifts $\mathbf{S}_1, \dots, \mathbf{S}_L$. This together with Assumption II.1 implies that \mathbf{P} is a diagonal matrix. The desired conclusion about the diagonal entries of the diagonal matrix \mathbf{P} then follows from its orthogonality property.

With the uniqueness property of the orthogonal matrix \mathbf{U} to diagonalize graph shifts $\mathbf{S}_1, \dots, \mathbf{S}_L$ simultaneously, we define the *graph Fourier transform* (GFT) $\widehat{\mathbf{x}} := \mathcal{F}\mathbf{x}$ of a graph signal \mathbf{x} by

$$\widehat{\mathbf{x}} = \mathbf{U}^T \mathbf{x}. \quad (\text{II.5})$$

Analogous to the classical discrete Fourier transform, we may use interpret the joint spectrum $\mathbf{\Lambda}$ of graph shifts $\mathbf{S}_1, \dots, \mathbf{S}_L$ as the set of frequencies to the above GFT, and their eigenvectors $\mathbf{u}_1, \dots, \mathbf{u}_N$ to form its graph Fourier basis [8], [10], [12], [13], [24], [40], [41], [42], [43].

For the GFT in (II.5), we obtain from the orthogonality property of the matrix \mathbf{U} in (II.2) that the following Parseval identity

$$\|\mathcal{F}\mathbf{x}\|_2 = \|\mathbf{x}\|_2$$

holds for every graph signal \mathbf{x} . By (II.2), the graph shift operation in the spatial domain is a multiplier in the Fourier domain. In particular, for any graph signal \mathbf{x} , the Fourier transform of its shifted signal $\mathbf{S}_l \mathbf{x}$ is the Hadamard product of the Fourier transform of the original signal \mathbf{x} and the vector of eigenvalues of the graph shift \mathbf{S}_l ,

$$\widehat{\mathbf{S}_l \mathbf{x}} = \mathbf{\Lambda}_l \widehat{\mathbf{x}}, \quad 1 \leq l \leq L, \quad (\text{II.6})$$

where $\mathbf{\Lambda}_l$ are diagonal matrices in (II.2).

III. GRAPH SHIFT-INVARIANT SPACES AND BANDLIMITED SPACES

Let \mathcal{G} be an undirected graph of order $N \geq 1$, and $\mathbf{S}_1, \dots, \mathbf{S}_L$ be commutative graph shifts on \mathcal{G} . We say that a linear space H of graph signals on \mathcal{G} is *shift-invariant* if

$$\mathbf{S}_l \mathbf{x} \in H \quad \text{for all } \mathbf{x} \in H \text{ and } 1 \leq l \leq L, \quad (\text{III.1})$$

and *bandlimited* if

$$H = B_\Omega \quad (\text{III.2})$$

for some $\Omega \subset \{1, \dots, N\}$, where

$$B_\Omega = \{\mathbf{x} \mid \text{supp } \widehat{\mathbf{x}} \subset \Omega\}. \quad (\text{III.3})$$

The bandlimited spaces B_Ω , also known as Paley-Wiener spaces, have been widely used in graph signal processing, see [14], [15], [16], [17], [18], [19] and references therein.

Let Φ be a nonempty set of nonzero graph signals on the graph \mathcal{G} , and set $\mathbf{S}^\alpha = \mathbf{S}_1^{\alpha_1} \dots \mathbf{S}_L^{\alpha_L}$ for $\alpha = [\alpha_1, \dots, \alpha_L]^T \in \mathbb{Z}_+^L$. We say that a graph shift-invariant space (GSIS) H is *generated* by Φ if it is the minimal shift-invariant space containing Φ , i.e.,

$$H = H(\Phi) := \text{span}\{\mathbf{S}^\alpha \phi \mid \alpha \in \mathbb{Z}_+^L, \phi \in \Phi\} \quad (\text{III.4})$$

and that H is *principal* if it is generated by a one graph signal. As $H(\Phi)$ is a linear subspace of \mathbb{R}^N , we may assume that Φ has finite cardinality. By the classical Cayley-Hamilton theorem, for every $1 \leq l \leq L$, \mathbf{S}_l^N is the linear combination of \mathbf{S}_l^m , $0 \leq m \leq N-1$. Therefore the GSIS generated by Φ is given by

$$H(\Phi) = \text{span}\{\mathbf{S}_1^{\alpha_1} \dots \mathbf{S}_L^{\alpha_L} \phi \mid 0 \leq \alpha_1, \dots, \alpha_L \leq N-1, \phi \in \Phi\}. \quad (\text{III.5})$$

In the classical real-line setting, a bandlimited space is a principal shift-invariant space and a principal shift-invariant space is shift-invariant, while the converse does not hold in general. In the following theorem, we show that the terminologies on bandlimitedness, shift-invariance, principal-shift-invariance are essentially the same in the undirected finite graph setting.

Theorem III.1. *Let \mathcal{G} be an undirected finite graph, and $\mathbf{S}_1, \dots, \mathbf{S}_L$ be graph shifts satisfying Assumption II.1, and H be a linear space of graph signals on the graph \mathcal{G} . Then the following statements are equivalent.*

- (i) H is a bandlimited space B_Ω for some $\Omega \subset \{1, \dots, N\}$.
- (ii) H is shift-invariant.
- (iii) H is a finitely-generated shift-invariant space (FGSIS).
- (iv) H is a principal shift-invariant space (PGSIS).

We divide the proof into the following steps: (iv) \implies (iii) \implies (ii) \implies (i) \implies (iv); see Appendix VII-A for the detailed proof. In the proof of the implication (ii) \implies (i), we show that a GSIS H is the bandlimited space B_Ω with

$$\Omega = \cup_{\mathbf{x} \in H} \text{supp } \widehat{\mathbf{x}} \quad \text{and} \quad \#\Omega = \dim H, \quad (\text{III.6})$$

where the second conclusion on the cardinality of the supporting set Ω holds as the bandlimited space B_Ω has dimension $\#\Omega$.

For the case that H is a GSIS generated by Φ , we obtain from (II.6) that for any $\alpha_1, \dots, \alpha_L \in \mathbb{Z}_+$ and $\phi \in \Phi$, the Fourier transform of $\mathbf{S}_1^{\alpha_1} \dots \mathbf{S}_L^{\alpha_L} \phi$ has its supported contained in the supporting set of $\widehat{\phi}$, i.e.,

$$\text{supp } \mathcal{F}(\mathbf{S}_1^{\alpha_1} \dots \mathbf{S}_L^{\alpha_L} \phi) = \text{supp } \mathbf{\Lambda}_1^{\alpha_1} \dots \mathbf{\Lambda}_L^{\alpha_L} \widehat{\phi} \subset \text{supp } \widehat{\phi}.$$

Therefore the set Ω in the bandlimited space $H = B_\Omega$ is completely determined by the generator Φ ,

$$\Omega = \cup_{\phi \in \Phi} \text{supp } \widehat{\phi}. \quad (\text{III.7})$$

The implication (i) \implies (iv) follows from the following theorem, see Appendix VII-B for the proof.

Theorem III.2. *Let \mathcal{G} be an undirected finite graph, and $\mathbf{S}_1, \dots, \mathbf{S}_L$ be graph shifts satisfying Assumption II.1. Then the bandlimited space B_Ω is generated by some graph signal $\phi_0 \in B_\Omega$ satisfying*

$$\widehat{\phi}_0(n) \neq 0 \text{ if and only if } n \in \Omega, \quad (\text{III.8})$$

and a graph shift \mathbf{T} , which is a linear combination of graphs shifts $\mathbf{S}_1, \dots, \mathbf{S}_L$, i.e.,

$$B_\Omega = \text{span}\{\mathbf{T}^m \phi_0 \mid 0 \leq m \leq \#\Omega - 1\}. \quad (\text{III.9})$$

We remark that the requirement (III.8) for the generator ϕ_0 is also a necessary condition for (III.9) to hold. Let χ_Ω be the characteristic function on the set Ω whose n -th component takes value one for every $n \in \Omega$ and value zero for any $n \notin \Omega$. Similar to the sinc function for the classical bandlimited space on the real line, our illustrative example of the generator ϕ_0 in (III.9) for the bandlimited space B_Ω is the graph signal $\mathcal{F}^{-1}\chi_\Omega$, the inverse Fourier transform of the characteristic function χ_Ω on the set Ω .

The linear combination requirement for the graph shift \mathbf{T} in Theorem III.2 can be relaxed to the commutativity property between \mathbf{T} and the graph shifts $\mathbf{S}_1, \dots, \mathbf{S}_L$. Under the above commutativity assumption, there exists a diagonal matrix $\mathbf{\Lambda}_\mathbf{T} = \text{diag}[\lambda_\mathbf{T}(1), \dots, \lambda_\mathbf{T}(N)]$ by Assumption II.1 such that

$$\mathbf{T} = \mathbf{U}\mathbf{\Lambda}_\mathbf{T}\mathbf{U}^T \quad (\text{III.10})$$

where \mathbf{U} is the orthogonal matrix in (II.1), see Proposition II.2. From the proof of Theorem III.2, we notice that a graph shift \mathbf{T} can be used in (III.9) if and only if $\lambda_\mathbf{T}(n), n \in \Omega$, are distinct.

A. Riesz bases for principal shift-invariant spaces

For the generator ϕ_0 and the graph shift \mathbf{T} of the bandlimited space B_Ω chosen in (III.9), we define

$$\mathbf{V}_\mathbf{T} = [(\lambda_\mathbf{T}(n))^m]_{n \in \Omega, 0 \leq m \leq \#\Omega - 1} \quad (\text{III.11})$$

and

$$\mathbf{V}_{\mathbf{T}, \phi_0} = [\widehat{\phi}_0(n)(\lambda_\mathbf{T}(n))^m]_{n \in \Omega, 0 \leq m \leq \#\Omega - 1}, \quad (\text{III.12})$$

where $\lambda_\mathbf{T}(n), n \in \Omega$ are given in (III.10), and $\widehat{\phi}_0(n), n \in \Omega$, are the n -th component of the Fourier transform $\widehat{\phi}_0$ of the generator ϕ_0 . By Theorem III.2, $\{\mathbf{T}^m \phi_0 \mid 0 \leq m \leq \#\Omega - 1\}$ is a Riesz basis for the bandlimited space B_Ω . Applying Parseval's identity for the GFT, we have the following Riesz bound estimate.

Proposition III.3. *Let the graph \mathcal{G} , the graph shifts $\mathbf{S}_1, \dots, \mathbf{S}_L$ and \mathbf{T} , the bandlimited space B_Ω , and the generator ϕ_0 be as in Theorem III.2. Then the minimal and maximal singular values of the matrix $\mathbf{V}_{\mathbf{T}, \phi_0}$ in (III.12) are the low and upper Riesz basis bounds of $\{\mathbf{T}^m \phi_0 \mid 0 \leq m \leq \#\Omega - 1\}$ of the bandlimited space B_Ω respectively, i.e.,*

$$\sigma_{\min}(\mathbf{V}_{\mathbf{T}, \phi_0}) \|\mathbf{c}\|_2 \leq \left\| \sum_{m=0}^{\#\Omega - 1} c_m \mathbf{T}^m \phi_0 \right\|_2 \leq \sigma_{\max}(\mathbf{V}_{\mathbf{T}, \phi_0}) \|\mathbf{c}\|_2 \quad (\text{III.13})$$

hold for all sequences $\mathbf{c} = [c_m]_{0 \leq m \leq \#\Omega - 1}$.

We remark that $\mathbf{V}_{\mathbf{T}, \phi_0}$ in (III.12) can be considered a weighted version of the Vandermonde matrix $\mathbf{V}_\mathbf{T}$ in (III.11), and their minimal/maximal singular values are related by

$$\left(\min_{n \in \Omega} |\widehat{\phi}_0(n)| \right) \sigma_{\min}(\mathbf{V}_\mathbf{T}) \leq \sigma_{\min}(\mathbf{V}_{\mathbf{T}, \phi_0}) \leq \sigma_{\max}(\mathbf{V}_{\mathbf{T}, \phi_0}) \leq \left(\max_{n \in \Omega} |\widehat{\phi}_0(n)| \right) \sigma_{\max}(\mathbf{V}_\mathbf{T}). \quad (\text{III.14})$$

Therefore we may use the minimal/maximal singular values of the Vandermonde matrix $\mathbf{V}_\mathbf{T}$ in (III.11) to estimate lower/upper bounds for the Riesz basis $\{\mathbf{T}^m \phi_0 \mid 0 \leq m \leq \#\Omega - 1\}$ of the bandlimited space B_Ω .

B. Frames for principal graph shift-invariant spaces

As a consequence of Theorems III.1 and III.2, every GSIS H is generated by finite shifts of some generator ϕ_0 , i.e.,

$$H = \text{span}\{\mathbf{S}^\alpha \phi_0 \mid \alpha \in \Sigma_{M-1}\} \quad (\text{III.15})$$

hold for all $M \geq \dim H$, where

$$\Sigma_M = \{[\alpha_1, \dots, \alpha_L]^T \in \mathbb{Z}_+^L \mid \alpha_1 + \dots + \alpha_L \leq M\}, \quad M \geq 1.$$

Unlike one graph shift scenario (i.e., $L = 1$), $\{\mathbf{S}^\alpha \phi_0 \mid \alpha \in \Sigma_{M-1}\}$ with $M \geq \dim H$ is not necessarily a basis for the shift-invariant space H when $L \geq 2$, however by (II.2) and (III.15), we see that it forms a frame for the GSIS H . Define

$$\mathbf{F}_M := [\mathbf{S}^\alpha \phi_0]_{\alpha \in \Sigma_{M-1}} \quad (\text{III.16})$$

and

$$\widehat{\mathbf{F}}_{M, \phi_0} = [(\boldsymbol{\lambda}(n))^\alpha \widehat{\phi}_0(n)]_{1 \leq n \leq N, \alpha \in \Sigma_{M-1}}, \quad (\text{III.17})$$

where $\widehat{\phi}_0(n)$ and $\boldsymbol{\lambda}(n)$, $1 \leq n \leq N$, of the n -th component of the Fourier transform $\widehat{\phi}_0$ of the generator ϕ_0 and the joint spectrum $\boldsymbol{\Lambda}$ of the graph shifts $\mathbf{S}_1, \dots, \mathbf{S}_L$ given in (II.3), respectively. Then one may verify that

$$\mathbf{F}_M = \mathbf{U} \widehat{\mathbf{F}}_{M, \phi_0}, \quad (\text{III.18})$$

where \mathbf{U} is the orthogonal matrix in (II.2). Then applying the Parseval identity for the GFT, we have the following frame bound estimate.

Proposition III.4. *Let the graph \mathcal{G} , graph shifts $\mathbf{S}_1, \dots, \mathbf{S}_L$, and the generator ϕ_0 be as in (III.15). Then the minimal nonzero singular value $\sigma_{\min}^+(\widehat{\mathbf{F}}_{M, \phi_0})$ and maximal singular value $\sigma_{\max}(\widehat{\mathbf{F}}_{M, \phi_0})$ of the matrix $\widehat{\mathbf{F}}_{M, \phi_0}$ in (III.17) are the low and upper frame bounds of the frame $\{\mathbf{S}^\alpha \phi_0 \mid \alpha \in \Sigma_{M-1}\}$ of the shift-invariant space H for all $M \geq \dim H$, i.e.,*

$$\sigma_{\min}^+(\widehat{\mathbf{F}}_{M, \phi_0}) \|\mathbf{x}\|_2 \leq \left(\sum_{\alpha \in \Sigma_{M-1}} |\langle \mathbf{x}, \mathbf{S}^\alpha \phi_0 \rangle|^2 \right)^{1/2} \leq \sigma_{\max}(\widehat{\mathbf{F}}_{M, \phi_0}) \|f\|_2, \quad \mathbf{x} \in H. \quad (\text{III.19})$$

C. Uncertainty principle for principal graph shift-invariant spaces

The generator ϕ_0 selected in (III.15) is more like the sinc function in the classical Paley-Wiener space. In this subsection, we show that a PGSIS generated by a well-localized graph signal does not have small dimension, see Proposition III.5.

For the orthogonal matrix $\mathbf{U} = [u_n(i)]_{1 \leq n \leq N, i \in V}$ in (II.2), define

$$\|\mathbf{U}\|_\infty = \sup_{1 \leq n \leq N, i \in V} |u_n(i)|$$

and

$$\|\mathbf{U}\|_\infty^* = \sup_{W \subset V, \Omega \subset \{1, \dots, N\}} \left\{ (\#W \# \Omega)^{-1/2} \mid \sum_{i \in W, n \in \Omega} |u_n(i)|^2 \geq 1 \right\}. \quad (\text{III.20})$$

Clearly, we have

$$N^{-1/2} \leq \|\mathbf{U}\|_\infty^* \leq \|\mathbf{U}\|_\infty. \quad (\text{III.21})$$

By the uncertainty principle in [44],

$$\#(\text{supp } \mathbf{x}) \times \#(\text{supp } \widehat{\mathbf{x}}) \geq (\|\mathbf{U}\|_\infty^*)^{-2} \quad (\text{III.22})$$

holds for all nonzero graph signals \mathbf{x} . The reader may refer to [44], [45], [46] and references therein for additional information on various graph uncertainty principle.

For a nonzero graph signal ϕ_0 , we obtain from (III.7) that the PGSIS generated by ϕ_0 is a bandlimited space B_Ω with $\Omega = \text{supp } \widehat{\phi}_0$. Then we conclude from (III.22) and the above observation that a PGSIS generated by a localized graph signal has higher dimension.

Proposition III.5. Let the graph \mathcal{G} and the graph shifts $\mathbf{S}_1, \dots, \mathbf{S}_L$ be as in Theorem III.2. Let ϕ_0 be a nonzero graph signal with its support denoted by W , and denote the PGSIS generated by ϕ_0 by $H(\phi_0)$. Then

$$\#W \times \dim H(\phi_0) \geq (\|\mathbf{U}\|_\infty^*)^{-2} \quad (\text{III.23})$$

where $\|\mathbf{U}\|_\infty^*$ is given in (III.20).

We finish this subsection with a remark on the optimality of the low bound estimate (III.23) for the PGSIS generated by a localized signal on a circulant graph.

Remark III.6. Let $1 \leq q_1 < \dots < q_L < N/2$ such that q_1, \dots, q_L, N being co-prime, and $\mathcal{C}(N, Q) = (V_N, E_N(Q))$ be the unweighted circulant graph generated by $Q := \{q_1, \dots, q_L\}$ that has the vertex set $V_N = \{0, 1, \dots, N-1\}$ and the edge set $E_N(Q) = \{(i, i \pm q \bmod N), i \in V_N, q \in Q\}$. Define $\mathbf{S}_l = (S_l(i, j))_{i, j \in V_N}$, $1 \leq l \leq L$, with $S_l(i, j) = 1$ if $j = i$, $S_l(i, j) = -1/2$ if $i - j = \pm q_l \bmod N$ and $S_l(i, j) = 0$ otherwise. One may verify that \mathbf{S}_l , $1 \leq l \leq L$, are commutative graph shifts. Denote the orthogonal matrix to diagonalize those graph shifts on the circulant graph $\mathcal{C}(N, Q)$ by $\mathbf{U}_{N, Q}$. For the above orthogonal matrix, we have

$$N^{-1/2} \leq \|\mathbf{U}_{N, Q}\|_\infty^* \leq \|\mathbf{U}_{N, Q}\|_\infty \leq 2^{1/2} N^{-1/2}, \quad (\text{III.24})$$

see [42, Section 6.1]. This indicates that the order $N^{-1/2}$ in the lower bound estimate in (III.21) is optimal for the orthogonal matrix $\mathbf{U}_{N, Q}$.

Let ϕ_0 be the delta signal supported at vertex $\lfloor N/2 \rfloor + 1$, where $\lfloor t \rfloor$ is the integral part of a real number t . One may verify that the GSIS space $H(\phi_0)$ contains all graph signals $\mathbf{x} = [x(0), \dots, x(N-1)]^T$ satisfying the following symmetry property:

$$x(\lfloor N/2 \rfloor - i) = x(\lfloor N/2 \rfloor + i), \quad 1 \leq i \leq N - 1 - \lfloor N/2 \rfloor,$$

and it has dimension $\lfloor N/2 \rfloor + 1$. Therefore, for the GSIS $H(\phi_0)$ on the circulant graph $\mathcal{C}(N, Q)$, the estimate in (III.23) becomes **accurate** when N is odd, and the difference between the left and right hand sides in (III.23) is at most one for even N .

IV. SHIFT-INVARIANT GRAPH REPRODUCING KERNEL HILBERT SPACES

Let $\mathbf{S}_1, \dots, \mathbf{S}_L$ be graph shifts on an undirected graph \mathcal{G} of order N , and H be a reproducing kernel Hilbert space (RKHS) of graph signals on \mathcal{G} . We say that its reproducing kernel \mathbf{K} is *shift-invariant* if it commutes with graph shifts $\mathbf{S}_1, \dots, \mathbf{S}_L$:

$$\mathbf{S}_l \mathbf{K} = \mathbf{K} \mathbf{S}_l, \quad 1 \leq l \leq L. \quad (\text{IV.1})$$

RKHSs with shift-invariant kernel (SIGRKHSs) have been widely used and appreciated in machine learning for function estimation on networks, and their popularity can be ascribed to their simplicity to represent functions, flexibility to select kernels, and efficiency to learn functions with low computational costs. By Proposition II.2, a shift-invariant reproducing kernel \mathbf{K} is a polynomial of graph shifts $\mathbf{S}_1, \dots, \mathbf{S}_L$. Common selection of shift-invariant kernels include the diffusion kernels $\exp(\sigma^2 \mathbf{L}^{\text{sym}}/2)$ with $\sigma > 0$, the p -step random walk kernels $(a\mathbf{I} - \mathbf{L}^{\text{sym}})^{-p}$ with $a > 2$ and $p \geq 1$, the Laplacian regularization kernels $\mathbf{I} + \sigma^2 \mathbf{L}^{\text{sym}}$ with $\sigma > 0$, and the spline kernels $((\mathbf{L}^{\text{sym}})^\dagger)^\alpha$, where $(\mathbf{L}^{\text{sym}})^\dagger$ is pseudo-inverse of the symmetrically normalized Laplacian \mathbf{L}^{sym} on the graph \mathcal{G} [8], [25], [26], [27], [28], [29], [30], [31], [32], [33], [34], [35].

For a SIGRKHS H with a shift-invariant kernel \mathbf{K} , we can express any element in H as a linear combination of the columns of \mathbf{K} , i.e.,

$$H = \{\mathbf{K}\mathbf{c}, \mathbf{c} \in \mathbb{R}^N\}. \quad (\text{IV.2})$$

The RKHS with a spline kernel $((\mathbf{L}^{\text{sym}})^\dagger)^p$, $p \geq 1$, are known as graph spline space in [33]. For the case that all eigenvalues of the symmetrically normalized Laplacian \mathbf{L}^{sym} are distinct (i.e., Assumption II.1 holds), one may verify that the RKHS associated with the diffusion kernels, the p -step random walk kernels, and the Laplacian regularization kernels are the whole Euclidean space \mathbb{R}^N with different inner products embedded.

By (IV.1) and (IV.2), we observe that a SIGRKHS H is a GSIS. In the following theorem, we show that the converse holds too, see Appendix VII-C for the proof.

Theorem IV.1. *Let \mathcal{G} be an undirected finite graph, and $\mathbf{S}_1, \dots, \mathbf{S}_L$ be graph shifts satisfying Assumption II.1. Then a GSIS H embedded with the standard Euclidean inner product is a SIGRKHS.*

From the proof of Theorem IV.1, we observe that the inner product $\langle \mathbf{x}, \mathbf{y} \rangle = \mathbf{x}^T \mathbf{y}$ of two graph signals \mathbf{x} and $\mathbf{y} \in H$ can be represented in the Fourier domain as follows:

$$\langle \mathbf{x}, \mathbf{y} \rangle = \widehat{\mathbf{x}}^T \mathbf{\Lambda}_\Omega \widehat{\mathbf{y}}, \quad (\text{IV.3})$$

where $\Omega \subset \{1, \dots, N\}$ is the set given in Theorem III.1 and $\mathbf{\Lambda}_\Omega = \text{diag}[\chi_\Omega(1), \dots, \chi_\Omega(N)]$ is the diagonal matrix with $\chi_\Omega(n) = 1$ for $n \in \Omega$ and $\chi_\Omega(n) = 0$ otherwise. In the following theorem, we show that the inner product of any SIGRKHS can be defined by a generalized dot product in the Fourier domain, see Appendix VII-D for the proof.

Theorem IV.2. *Let \mathcal{G} be an undirected finite graph, and $\mathbf{S}_1, \dots, \mathbf{S}_L$ be graph shifts satisfying Assumption II.1. Then a SIGRKHS H has its inner product defined by*

$$\langle \mathbf{x}, \mathbf{y} \rangle_H = \widehat{\mathbf{x}}^T \mathbf{B} \widehat{\mathbf{y}}, \quad \mathbf{x}, \mathbf{y} \in H, \quad (\text{IV.4})$$

where \mathbf{B} is a diagonal matrix with nonnegative diagonal entries.

Let \mathbf{K} be the shift-invariant kernel of a SIGRKHS H , $\Omega \subset \{1, \dots, N\}$ be as in Theorem III.1 and \mathbf{U} be the orthogonal matrix in (II.2). By (IV.1) and Proposition II.2, we observe that $\mathbf{K} = \mathbf{U} \mathbf{\Lambda}_\mathbf{K} \mathbf{U}^T$ for some diagonal matrix $\mathbf{\Lambda}_\mathbf{K}$ with its n -th entries taking positive value for $n \in \Omega$ and zero value otherwise. From the proof of Theorem IV.2, we observe that the pseudo-inverse $\mathbf{\Lambda}_\mathbf{K}^\dagger$ of the diagonal matrix $\mathbf{\Lambda}_\mathbf{K}$ can be used in (IV.4) to define the inner product of the SIGRKHS H . In particular, one may verify that a matrix \mathbf{B} with nonnegative diagonal entries can be used in (IV.4) if and only if $\mathbf{B} - \mathbf{\Lambda}_\mathbf{K}^\dagger$ has n -th diagonal entries taking zero value for all $n \in \Omega$.

Given a diagonal matrix \mathbf{B} with nonnegative diagonal entries, one may verify that the bandlimited space

$$B_{\Omega_B} = \{ \mathbf{x} \mid \text{supp } \widehat{\mathbf{x}} \subset \Omega_B \}$$

embedded with the inner product in (IV.4) is a RKHS with the shift-invariant kernel $\mathbf{U} \mathbf{B}^\dagger \mathbf{U}^T$, where Ω_B is the supporting set of diagonal entries of the diagonal matrix \mathbf{B} and \mathbf{B}^\dagger is the pseudo-inverse of the matrix \mathbf{B} .

Given a reproducing kernel space H with the inner product defined by (IV.4), we see that the evaluation functional is uniformly bounded, i.e.,

$$|x(i)| \leq \|\mathbf{x}\|_2 = \|\widehat{\mathbf{x}}\|_2 \leq \left(\min_{b(n) \neq 0} b(n) \right)^{-1/2} \|\mathbf{x}\|_H, \quad i \in V, \quad (\text{IV.5})$$

hold for all graph signals $\mathbf{x} = [x(i)]_{i \in V} \in H$, where $\mathbf{B} = \text{diag}(b(1), \dots, b(N))$ is the diagonal matrix in (IV.4).

V. SAMPLING AND RECONSTRUCTION IN A FINITELY-GENERATED GRAPH SHIFT-INVARIANT SPACE

Let $\mathbf{S}_1, \dots, \mathbf{S}_L$ be graph shifts on an undirected graph \mathcal{G} of order N , $H(\Phi)$ be the GSIS generated by $\Phi = \{\phi_0, \dots, \phi_{R-1}\}$. In this section, we consider linear sampling and reconstruction problem in the GSIS $H(\Phi)$,

$$S : H(\Phi) \ni \mathbf{x} \mapsto \mathbf{A} \mathbf{x}, \quad (\text{V.1})$$

where $\mathbf{A} = [a(s, i)]_{s \in W, i \in V}$ is the sampling matrix.

An illustrative example of the sampling scheme (V.1) is the ideal sampling on $W \subset V$, in which the sampling matrix is given by

$$\mathbf{A}_W = [a_W(i, j)]_{i \in W, j \in V} \quad (\text{V.2})$$

where $a_W(i, j) = 0$ except that $a_W(i, i) = 1, i \in W$. The above sampling scheme is also known as *subset sampling* [14], [15], [16], [17], [18], [19]. Another illustrative example of the sampling scheme (V.1) is *dynamic sampling* (also known as *aggregation sampling*),

$$S_{\mathbf{D}, i_0} : \mathbf{x} \mapsto [\mathbf{x}(i_0), (\mathbf{D}\mathbf{x})(i_0), \dots, (\mathbf{D}^{K-1}\mathbf{x})(i_0)] \quad (\text{V.3})$$

where $i_0 \in V, K \geq 1$, \mathbf{D} is the state matrix and $\mathbf{x}(i_0)$ is i_0 -th component of a graph signal \mathbf{x} [19], [47], [48], [49], [50].

For the sampling procedure in (V.1), we have the following characterization on its injectivity.

Theorem V.1. *Let \mathcal{G} be an undirected finite graph of order N , $\mathbf{S}_1, \dots, \mathbf{S}_L$ be graph shifts satisfying Assumption II.1, $H(\Phi)$ be the GSIS generated by $\Phi = \{\phi_0, \dots, \phi_{R-1}\}$, and set the frame matrix $\mathbf{F}_N = [\mathbf{S}^\alpha \phi]_{\alpha \in \Sigma_{N-1}, \phi \in \Phi}$. Then the sampling procedure (V.1) with sampling matrix \mathbf{A} is one-to-one if and only if \mathbf{F}_N and $\mathbf{A}\mathbf{F}_N$ have the same rank.*

Similar to (III.19) for PGSISs, we have that the columns of \mathbf{F}_N form a frame for $H(\Phi)$. Hence its rank is the same as the dimension of the GSIS $H(\Phi)$ and also the cardinality of the supporting set Ω of the corresponding bandlimited space in Theorem III.1,

$$\text{rank}(\mathbf{F}_N) = \dim H(\Phi) = \#\Omega. \quad (\text{V.4})$$

This together with the observation that dimension of the range space of the sampling operator S is the same as the rank of the matrix $\mathbf{A}\mathbf{F}_N$ proves the desired equivalence in Theorem V.1.

Let $\Omega \subset \{1, \dots, N\}$ and $\phi_0 \in B_\Omega$ be a nonzero signal with its GFT $\widehat{\phi}_0$ has its n -th component taking nonzero value for all $n \in \Omega$. Then the GSIS $H(\phi_0)$ generated by ϕ_0 is the bandlimited space B_Ω , i.e., $H(\phi_0) = \text{span}\{\mathbf{u}_n, n \in \Omega\}$, where $\mathbf{U} = [\mathbf{u}_1, \dots, \mathbf{u}_N]$ is the orthogonal matrix in (II.2). Combining the above observation with (V.4) and Theorem V.1, we obtain the following result on the uniqueness for subset sampling on bandlimited spaces.

Corollary V.2. *Let \mathcal{G} be an undirected graph of order N , $\mathbf{S}_1, \dots, \mathbf{S}_L$ be graph shifts satisfying Assumption II.1, and $\mathbf{U} = [u_n(i)]_{1 \leq n \leq N, i \in V}$ be the orthogonal matrix in (II.2). Then for any $\Omega \subset \{1, \dots, N\}$ and $W \subset V$, the ideal sampling of the bandlimited space B_Ω on the sampling set W is one-to-one if and only if the submatrix $[u_n(i)]_{n \in \Omega, i \in W}$ of the orthogonal matrix \mathbf{U} has rank $\#\Omega$.*

The conclusion in Corollary V.2 has been established in [14], [16], [19] and references therein for subset sampling on bandlimited spaces.

For the dynamic sampling (V.3) with the state matrix \mathbf{D} being commutative with graph shifts $\mathbf{S}_1, \dots, \mathbf{S}_L$, one may verify that the corresponding sampling matrix is given by

$$\mathbf{A}_{\mathbf{D}, i_0} = [(\lambda_{\mathbf{D}}(n))^k]_{0 \leq k \leq K-1, 1 \leq n \leq N} \text{diag}[u_1(i_0), \dots, u_N(i_0)] \mathbf{U},$$

where $\text{diag}[\lambda_{\mathbf{D}}(1), \dots, \lambda_{\mathbf{D}}(N)] = \mathbf{U}^T \mathbf{D} \mathbf{U}$, and $[u_1(i_0), \dots, u_N(i_0)]$ is the i_0 -th row of the orthogonal matrix. This together with Theorem V.1 yields the following result on the uniqueness of dynamic sampling scheme (V.3) on a GSIS.

Corollary V.3. *Let \mathcal{G} be an undirected graph of order N , $\mathbf{S}_1, \dots, \mathbf{S}_L$ be graph shifts satisfying Assumption II.1 and $H(\Phi)$ be the GSIS generated by a finite family Φ of graph signals, and consider the dynamic sampling scheme $S_{\mathbf{D}, i_0}$ on the GSIS $H(\Phi)$ at location $i_0 \in V$ with the state matrix \mathbf{D} commutative with graph shifts. Then the sampling procedure in (V.3) is one-to-one if and only if $K \geq \#\Omega$, $\lambda_{\mathbf{D}}(n), n \in \Omega$ are distinct, and $u_n(i_0) \neq 0$ for all $n \in \Omega$, where $\Omega \subset \{1, \dots, N\}$ is given in Theorem III.1.*

Next consider signal reconstruction associated with the sampling scheme (V.1) on the GSIS $H(\Phi)$, under the assumption that the sampling scheme (V.1) is one-to-one and the given observation data is the sampling of some signal $\mathbf{x}_0 \in H(\Phi)$ corrupted by some random/deterministic noise $\boldsymbol{\epsilon}$,

$$\mathbf{y} = \mathbf{A}\mathbf{x}_0 + \boldsymbol{\epsilon}. \quad (\text{V.5})$$

Let $\Omega \subset \{1, \dots, N\}$ be the set in Theorem III.1 so that $H(\Phi) = B_\Omega$ and set $\mathbf{U}_\Omega = [\mathbf{u}_n]_{n \in \Omega}$. Considering the GSIS $H(\Phi)$ as a bandlimited space, we may use

$$\mathbf{x}_0^\sharp = \mathbf{U}_\Omega (\mathbf{U}_\Omega^T \mathbf{A}^T \mathbf{A} \mathbf{U}_\Omega)^{-1} \mathbf{U}_\Omega^T \mathbf{A}^T \mathbf{y}, \quad (\text{V.6})$$

a solution of the minimization problem

$$\mathbf{x}_0^\sharp = \arg \min_{\mathbf{x} \in H(\Phi)} \|\mathbf{A}\mathbf{x} - \mathbf{y}\|_2,$$

as the reconstructed signal in $H(\Phi)$. We remark that $\mathbf{U}_\Omega^T \mathbf{A}^T \mathbf{A} \mathbf{U}_\Omega$ is invertible by the assumption that the sampling scheme (V.1) is one-to-one and its characterization in Theorem V.1. For the numerical implementation of the

reconstruction algorithm (V.6), we observe that $\mathbf{U}_\Omega^T \mathbf{A}^T \mathbf{y}$ is essentially the restriction of the Fourier transform of $\mathbf{A}^T \mathbf{y}$ onto the set Ω , and hence we may consider the reconstruction formula (V.6) for the sampling scheme (V.1) on a GSIS as an implementation in the Fourier domain.

For $1 \leq n \leq N$, define

$$H_n(\Phi) = \text{span}\{\mathbf{S}^\alpha \phi \mid \alpha \in \Sigma_n, \phi \in \Phi\}. \quad (\text{V.7})$$

We observe that the GSIS $H(\Phi)$ generated by Φ could be approximated successively by nested Krylov spaces,

$$\text{span}\{\Phi\} = H_0(\Phi) \subset H_1(\Phi) \subset \dots \subset H_{N-1}(\Phi) = H(\Phi). \quad (\text{V.8})$$

This inspires us to propose the following iterative algorithm with finite steps to recover the signal \mathbf{x}_0^\sharp in (V.6), where

$$\langle \mathbf{x}_1, \mathbf{x}_2 \rangle_{\mathbf{A}} = \mathbf{x}_1^T \mathbf{A}^T \mathbf{A} \mathbf{x}_2 \quad \text{and} \quad \|\mathbf{x}_1\|_{\mathbf{A}} = \sqrt{\langle \mathbf{x}_1, \mathbf{x}_1 \rangle_{\mathbf{A}}} \quad (\text{V.9})$$

for $\mathbf{x}_1, \mathbf{x}_2 \in \mathbb{R}^N$, see Algorithm V.1.

Algorithm V.1 Reconstruction algorithm for signals in a FGSIS

Input: N (order of the underlying graph), $\mathbf{S}_1, \dots, \mathbf{S}_L$ (commutative graph shifts), $\phi_0, \dots, \phi_{R-1}$ (generators of the FGSIS), \mathbf{A} (the sampling matrix), $\mathbf{y} = \mathbf{A}\mathbf{x}_0 + \mathbf{e}$ (the noisy observation of some signal $\mathbf{x}_0 \in H(\phi_0, \dots, \phi_{R-1})$), and sampling error threshold δ .

Initial: Perform Gram-Schmidt process to $\phi_0, \dots, \phi_{R-1}$ with respect to the inner product $\langle \cdot, \cdot \rangle_{\mathbf{A}}$, and obtain an orthonormal basis \mathbf{W}_0 . Set $d_0 = \#\mathbf{W}_0$, $\mathbf{W}_0 = \{\mathbf{w}_1, \dots, \mathbf{w}_{d_0}\}$ and $\mathbf{W}_{-1} = \emptyset$. Define $\mathbf{x} = \sum_{m=1}^{d_0} \langle \mathbf{y}, \mathbf{A}\mathbf{w}_m \rangle \mathbf{w}_m$ and $\mathbf{e} = \mathbf{y} - \mathbf{A}\mathbf{x}$.

If $\|\mathbf{e}\|_2 \leq \delta$, set $\mathbf{x}_{\text{out}} = \mathbf{x}$, $\mathbf{e}_{\text{final}} = \mathbf{e}$, $D = 0$, and stop, else do the following iteration.

Iteration:

for $n = 1 : N - 1$

- a) Set $\mathbf{v}_{l,m'} = \mathbf{S}_l \mathbf{w}_{m'} - \sum_{m=1}^{d_{n-1}} \langle \mathbf{S}_l \mathbf{w}_{m'}, \mathbf{w}_m \rangle_{\mathbf{A}} \mathbf{w}_m$ for all $1 \leq l \leq L$ and $\mathbf{w}_{m'} \in \mathbf{W}_{n-1} \setminus \mathbf{W}_{n-2}$.
- b) If $\mathbf{v}_{l,m'} = 0$ for all $1 \leq l \leq L$ and $\mathbf{w}_{m'} \in \mathbf{W}_{n-1} \setminus \mathbf{W}_{n-2}$, then set $\mathbf{x}_{\text{out}} = \mathbf{x}$, $\mathbf{e}_{\text{final}} = \mathbf{e}$, $D = n - 1$ and stop.
- c) Else perform Gram-Schmidt process to $\{\mathbf{v}_{l,m'} \mid 1 \leq l \leq L, \mathbf{w}_{m'} \in \mathbf{W}_{n-1} \setminus \mathbf{W}_{n-2}\}$ with respect to the inner product $\langle \cdot, \cdot \rangle_{\mathbf{A}}$, and obtain an orthonormal basis $\widetilde{\mathbf{W}}_n$.
- d) Set $d_n = d_{n-1} + \#\widetilde{\mathbf{W}}_n$, write $\widetilde{\mathbf{W}}_n = \{\mathbf{w}_{d_{n-1}+1}, \dots, \mathbf{w}_{d_n}\}$, and update $\mathbf{W}_n = \mathbf{W}_{n-1} \cup \widetilde{\mathbf{W}}_n$.
- e) Set $\mathbf{z} = \sum_{m=d_{n-1}+1}^{d_n} \langle \mathbf{e}, \mathbf{A}\mathbf{w}_m \rangle \mathbf{w}_m$, $\mathbf{x} = \mathbf{x} + \mathbf{z}$ and $\mathbf{e} = \mathbf{e} - \mathbf{A}\mathbf{z}$.
- f) If $\|\mathbf{e}\|_2 \leq \delta$, set $\mathbf{x}_{\text{out}} = \mathbf{x}$, $\mathbf{e}_{\text{final}} = \mathbf{e}$, $D = n$ and stop, else continue the loop.

end

Output: The reconstruction signal \mathbf{x}_{out} , the sampling error $\mathbf{e}_{\text{final}} = \|\mathbf{y} - \mathbf{A}\mathbf{x}_{\text{out}}\|$, and the degree D of graph shifts to represent the reconstructed signal \mathbf{x}_{out} .

By the one-to-one property of the sampling scheme (V.1), we obtain from Theorem V.1 that $\langle \cdot, \cdot \rangle_{\mathbf{A}}$ in (V.9) defines an inner product on $H(\Phi)$. For the iteration section of Algorithm V.1, one may verify by induction that in step a), $\langle \mathbf{v}_{l,m'}, \mathbf{w}_m \rangle_{\mathbf{A}} = 0$ for all $1 \leq l \leq L$, $\mathbf{w}_{m'} \in \mathbf{W}_{n-1} \setminus \mathbf{W}_{n-2}$ and $\mathbf{w}_m \in \mathbf{W}_{n-1}$; in step d), $d_n = \dim H_n(\Phi)$, $\|\mathbf{w}_m\|_{\mathbf{A}} = 1$ if $1 \leq m \leq d_n$, $\langle \mathbf{w}_m, \mathbf{w}_{m'} \rangle_{\mathbf{A}} = 1$ for all $1 \leq m \neq m' \leq d_n$, and

$$H_n(\Phi) = \text{span}\{\mathbf{w}_m, 1 \leq m \leq d_n\}; \quad (\text{V.10})$$

and in step e), the reconstruction signal \mathbf{x} is the solution of the following minimization

$$\mathbf{x}_n := \arg \min_{\mathbf{w} \in \text{span} \widetilde{\mathbf{W}}_n} \|\mathbf{e} - \mathbf{A}\mathbf{w}\|_2 = \arg \min_{\mathbf{x} \in H_n(\Phi)} \|\mathbf{y} - \mathbf{A}\mathbf{x}\|_2. \quad (\text{V.11})$$

As the consequence of the above observations, the output $\mathbf{x}_{\text{out}} \in H(\Phi)$ of Algorithm V.1 is either a graph signal to match the noisy data \mathbf{y} within the threshold δ in the sense that

$$\|\mathbf{y} - \mathbf{A}\mathbf{x}_{\text{out}}\|_2 \leq \delta,$$

or the graph signal \mathbf{x}_0^\sharp in (V.6) that has least approximation error

$$\|\mathbf{y} - \mathbf{A}\mathbf{x}_{\text{out}}\|_2 = \min_{\mathbf{x} \in H(\Phi)} \|\mathbf{y} - \mathbf{A}\mathbf{x}\|_2.$$

Comparing with the reconstruction algorithm (V.6) for the sampling scheme (V.1), we may consider the proposed Algorithm V.1 as a reconstruction scheme in the spatial domain. In the next section, we will demonstrate the performance of the above algorithm to reconstruct well-localized signals in the spatial domain.

Remark V.4. For the orthonormal basis $\mathbf{w}_m, 1 \leq m \leq d_D$, constructed in Algorithm V.1, we obtain from (V.10) that for any $\mathbf{w}_m \in \mathbf{W}_n \setminus \mathbf{W}_{n-1}, 0 \leq n \leq D$, there exist polynomials $p_{m,r}, 0 \leq r \leq R-1$, of degree n such that

$$\mathbf{w}_m = \sum_{r=0}^{R-1} p_{m,r}(\mathbf{S}_1, \dots, \mathbf{S}_L) \phi_r.$$

Under the scenario that the sampling matrix \mathbf{A} satisfies the requirement that $\mathbf{A}^T \mathbf{A}$ is commutative with the graph shifts, we can reformulate the inner product $\langle \mathbf{w}_m, \mathbf{w}_{m'} \rangle_{\mathbf{A}}$ between \mathbf{w}_m and $\mathbf{w}_{m'}, 1 \leq m, m' \leq d_D$, in the Fourier domain as follows:

$$\langle \mathbf{w}_m, \mathbf{w}_{m'} \rangle_{\mathbf{A}} = \sum_{k=1}^N p_{m,r}(\boldsymbol{\lambda}(k)) p_{m',r}(\boldsymbol{\lambda}(k)) |\widehat{\phi}_r(k)|^2 \mu_k, \quad (\text{V.12})$$

where $\boldsymbol{\lambda}(k), 1 \leq k \leq N$, are joint spectrum of the graph shifts $\mathbf{S}_1, \dots, \mathbf{S}_L$ given in (II.3) and $\mathbf{A}^T \mathbf{A} = \mathbf{U} \boldsymbol{\Lambda}_{\mathbf{A}^T \mathbf{A}} \mathbf{U}$ for some diagonal matrix $\boldsymbol{\Lambda}_{\mathbf{A}^T \mathbf{A}}$ with diagonal entries $\mu_k, 1 \leq k \leq N$. Under the additional assumption that there is only one graph shifts (i.e., $L = 1$), we have $d_n = n + 1$ for $0 \leq n \leq D$, and polynomials $p_{m,1}$ of degree m are orthogonal polynomials with respect to the discrete measure $d\mu = \sum_{k=1}^N |\widehat{\phi}_r(k)|^2 \mu_k \delta_{\boldsymbol{\lambda}(k)}$ supported on the spectrum of the graph shifts,

$$\langle \mathbf{w}_m, \mathbf{w}_{m'} \rangle_{\mathbf{A}} = \int_{\mathbb{R}} p_{m,1}(t) p_{m',1}(t) d\mu(t). \quad (\text{V.13})$$

Therefore the polynomials $p_{m,1}, 0 \leq m \leq D$, satisfies the following three-term recurrence relation of the form

$$p_{m,1}(t) = (A_m t + B_m) p_{m-1,1}(t) + C_m p_{m-2,1}, \quad 2 \leq m \leq D-1,$$

for some triple (A_m, B_m, C_m) determined by the discrete measure $d\mu$.

VI. NUMERICAL SIMULATIONS

In this section, we evaluate the performance of Algorithm V.1 in consideration of reconstruction problem (V.1) for damped cosine wave signals in a GSIS on circulant graphs from their noise samples and flight delay dataset of the 50 busiest airports in the USA.

A. GSIS signal reconstruction on circulant graphs

Let the undirected circulant graph $\mathcal{C}(N, Q)$ and the graph shifts $\mathbf{S}_l, 1 \leq l \leq L$, be as in Remark III.6. Take the delta signal ϕ_0 at the vertex $\lfloor N/2 \rfloor$ and consider the GSIS $H(\phi_0)$ generated by ϕ_0 . We observe that the GSIS $H(\phi_0)$ admits the successive Krylov approximation,

$$\text{span}\{\phi_0\} = H_0(\phi_0) \subseteq \dots \subseteq H_{N-1}(\phi_0) = H(\phi_0),$$

where Krylov spaces $H_n(\phi_0), n \geq 0$, are given by

$$H_n(\phi_0) = \text{span}\{\mathbf{S}_1^{\alpha_1} \dots \mathbf{S}_L^{\alpha_L} \phi_0 \mid [\alpha_1, \dots, \alpha_L] \in \Sigma_n\}. \quad (\text{VI.1})$$

On the circulant graph $\mathcal{C}(N, Q)$ with $N = 100$ and $Q = \{1, 3\}$, one may verify that the above Krylov spaces $H_n(\phi_0)$ in (VI.1) have dimension 1 for $n = 0$, $3n$ for $1 \leq n \leq \lfloor N/6 \rfloor = 16$, 50 for $n = 17$ and 51 for $n \geq 18$.

In this subsection, we consider sampling and reconstruction of the damped cosine wave signal $\mathbf{x}_0 = [x_0(i)]_{0 \leq i \leq N-1}$ on the circulant graph $\mathcal{C}(N, Q)$, where A is the amplitude, λ is the decay constant, ω is the angular frequency, and

$$x_0(i) = A e^{-\lambda|i-\lfloor N/2 \rfloor|} \cos(\omega|i-\lfloor N/2 \rfloor|), \quad 0 \leq i \leq N-1. \quad (\text{VI.2})$$

The above wave signals belong to the GSIS space $H(\phi_0)$ and are well-localized and symmetric around the vertex $\lfloor N/2 \rfloor$; see the top plots of Figure 1 in blue, where $N = 100$ and $Q = \{1, 3\}$. Moreover, one may verify that maximal relative approximation errors from the Krylov spaces $H_n(\phi_0)$ have exponential decay,

$$E_n := \inf_{\mathbf{x}_n \in H_n(\phi_0)} \frac{\|\mathbf{x}_0 - \mathbf{x}_n\|_{\infty}}{\|\mathbf{x}_0\|_{\infty}} \leq e^{-(3n-1)\lambda}, \quad 1 \leq n \leq \lfloor N/6 \rfloor. \quad (\text{VI.3})$$

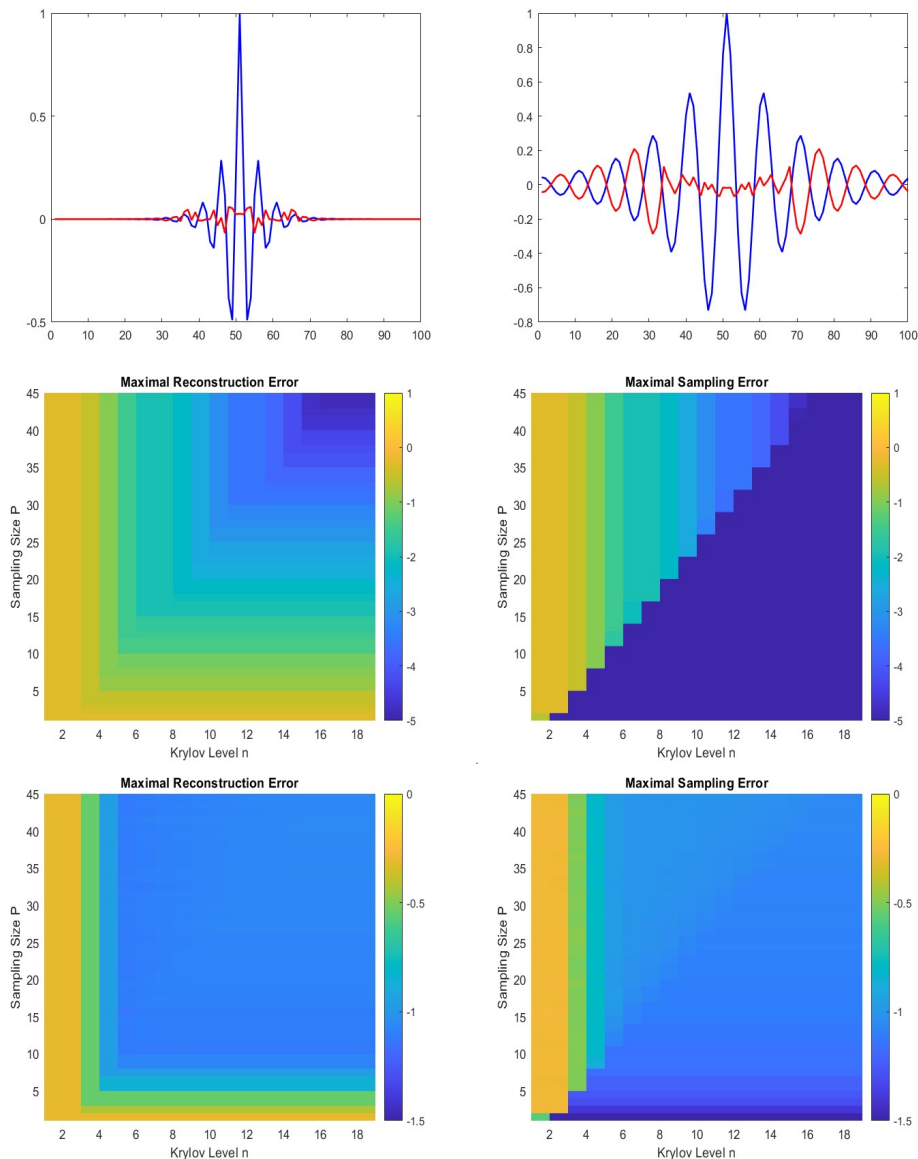


Fig. 1: Plotted on the top are the damped cosine wave signal \mathbf{x}_0 (in blue) and the reconstruction error $\mathbf{x}_{n,W} - \mathbf{x}_0$ (in red), where $A = 1, n = 6, N = 100, P = \lfloor N/6 \rfloor = 16, \sigma = 0.1$, and $(\lambda, \omega) = (1/4, 2\pi/5)$ (top left) and $(1/8, 2\pi/10)$ (top right). The relative maximal reconstruction error $\text{RE}(6, 16)$ and the relative maximal sampling error $\text{SE}(6, 16)$ are $(0.0680, 0.0680)$ (top left) and $(0.2865, 0.0679)$ (top right) respectively. Shown in the middle and bottom rows are the average of the relative maximal signal reconstruction error $\text{RE}(n, P)$ (left) and the relative maximal sampling error $\text{SE}(n, P)$ (right) over $M = 100$ trials, where $1 \leq n \leq 18, 1 \leq P \leq 45$, \mathbf{x}_0 is the damped cosine wave signal with $A = 1, \lambda = 1/4$ and $\omega = 2\pi/5$, and the noise level $\sigma = 0$ (the middle row) and $\sigma = 0.1$ (the bottom row).

In the simulations, we consider the subset sampling scheme (V.2) with the sampling set W being symmetric around $\lfloor N/2 \rfloor$, and the observation data \mathbf{y} is corrupted by some uniform random noises,

$$\mathbf{y}(i) = \mathbf{x}_0(i) + \epsilon(i), \quad i \in W_P,$$

where $W_P = \{\lfloor N/2 \rfloor - P, \dots, \lfloor N/2 \rfloor + P\}$ for some $P \geq 1$, and $\epsilon(i)_{i \in W_P}$ are i.i.d. random variables with uniform distribution on $[-\sigma, \sigma]$ for some $\sigma > 0$.

In the simulations, we use average of the relative maximal signal reconstruction error in the logarithmic scale,

$$\text{RE}(n, P) = \log_{10} \left(\frac{\|\mathbf{x}_{n,W_P} - \mathbf{x}_0\|_{\infty}}{\|\mathbf{x}_0\|_{\infty}} + 10^{-6} \right),$$

and the relative maximal sampling error in the logarithmic scale,

$$\text{SE}(n, P) = \log_{10} \left(\frac{\|\mathbf{A}_{W_P}(\mathbf{x}_{n, W_P} - \mathbf{x}_0)\|_\infty}{\|\mathbf{A}_{W_P} \mathbf{x}_0\|_\infty} + 10^{-6} \right)$$

over M trials to measure the performance of the Algorithm V.1, where $M \geq 1$, \mathbf{A}_{W_P} is the sampling matrix, and $\mathbf{x}_{n, W_P} \in H_n(\phi_0)$, $n \geq 0$, are signals reconstructed by Algorithm V.1 in its n -th iteration; see (V.11).

Presented in Figure 1 are the performances of Algorithm V.1 to reconstruct the damped cosine wave signals in (VI.2) from their noiseless and noisy samples. For the noiseless scenario shown in the middle row of Figure 1, we have the following observations for the relative maximal signal reconstruction error $\text{RE}(n, P)$ and the relative maximal sampling error $\text{SE}(n, P)$:

- 1) They decrease to zero when Krylov level n and sampling size W_P increase;
- 2) For any given sampling size $1 \leq P \leq \lfloor N/6 \rfloor$, they stay unchanged for $n \geq \lfloor (P+1)/3 \rfloor + 1$; and
- 3) For any fixed Krylov level $n \leq \lfloor N/3 \rfloor$, they take the same value for all $P \geq 3n$.

Therefore, for any given sampling size P , we may use $n_0 = \lfloor P/3 \rfloor + 1$ as the Krylov level instead of the default level $N-1$ in Algorithm V.1, see the top plots of Figure 1. Our numerical results also show that the maximal relative signal reconstruction error $\|\mathbf{x}_{n_0, W_P} - \mathbf{x}_0\|_\infty / \|\mathbf{x}_0\|_\infty$ is proportional to the best maximal approximation error E_n in (VI.3). The possible reasons we believe are that signals in the Krylov space $H_n(\phi)$ are supported in $[\lfloor N/2 \rfloor - 3n, \lfloor N/2 \rfloor + 3n]$ and they can be fully recovered from their samples on vertices in that interval.

For the noisy scenario shown in the bottom row of Figure 1, we observe that the relative maximal signal reconstruction error $\text{RE}(n, P)$ and the relative maximal sampling error $\text{SE}(n, P)$ have the same monotonic property about the Krylov level n and the sampling size P , however they do not improve significantly when $P \geq 12$ and $n \geq 5$. The possible reason is that the damped cosine wave function \mathbf{x}_0 is well-localized around $\lfloor N/2 \rfloor$ with $\sup_{|i - \lfloor N/2 \rfloor| \geq 13} |x_0(i)| = 0.0235$ and its noisy samples at vertices i with $|i - \lfloor N/2 \rfloor| \geq 13$ are dominated by random noises at level $\sigma = 0.1$.

B. Flight-delay dataset and graph shift-invariant spaces

Flight delays are inevitable especially for frequent flyers. In this subsection, we consider modeling arrival performance (measured as delays in minutes) of the top 50 airports out of 323 airports in the USA with the highest traffic volume [32], [51], and select the dataset on July, August, and September in 2014 and 2015 in our simulations for total 184 days, see the top left plot of Figure 2.

We model the flight delay dataset as a family of graph signals $\mathbf{x}_d = (x_d(n))_{n \in A}$, $1 \leq d \leq 184$, on the undirected graph $\mathcal{F} = (A, D)$, where d indicates the date in the dataset, the vertex set A has vertices indicating the top 50 airports and the edge set D contains all airport pairs so that the number of mutual flights between them exceeds 100 in the three months (roughly one direct flight between them per day). The underlying graph is designed to ensure that our analysis focuses on the busiest and most significant hubs, which are likely to have a greater influence on overall air traffic patterns and network dynamics. In the simulations, we use the corresponding symmetrically normalized graph Laplacian \mathbf{L}^{sym} as the graph shift in the definition of our proposed GSIS and bandlimiting model.

Three most common causes of flight delay are extreme weather condition, air traffic congestion and technical issues by operating airlines. The first two sources may lead to delay of most flights leaving and landing at the airports in certain region, while the last reason may create a ripple effect for flights operated by the airline at its hub airports. In our simulations, we consider nonadaptive GSIS

$$H = \text{span}\{(\mathbf{L}^{\text{sym}})^n \delta_i \mid n \geq 0, 1 \leq i \leq 3\}$$

and adaptive GSISs

$$H_d = \text{span}\{(\mathbf{L}^{\text{sym}})^n \delta_{i,d} \mid n \geq 0, 1 \leq i \leq 3\}, \quad 1 \leq d \leq 184,$$

to model graph signals \mathbf{x}_d , $1 \leq d \leq 184$, where δ_i and $\delta_{i,d}$, $1 \leq i \leq 3$, are delta signals at vertices representing airports with top three delay on average in the dataset and at day d , $1 \leq d \leq 184$, respectively. Let H_n and $H_{d,n}$, $0 \leq n \leq 49$, be the corresponding Krylov spaces spanned by $(\mathbf{L}^{\text{sym}})^m \delta_i$ and $(\mathbf{L}^{\text{sym}})^m \delta_{i,d}$ with $0 \leq m \leq n$, $1 \leq i \leq 3$ respectively. Shown at the bottom left plot of Figure 2 is the average of (non)adaptive maximal Krylov approximation error and bandlimiting approximation error,

$$F_{K,n} = \|\mathbf{x}_d - \mathbf{x}_{K;d,n}\|_\infty \quad \text{and} \quad F_{B,n} = \|\mathbf{x}_d - \mathbf{x}_{B;d,n}\|_\infty \quad (\text{VI.4})$$

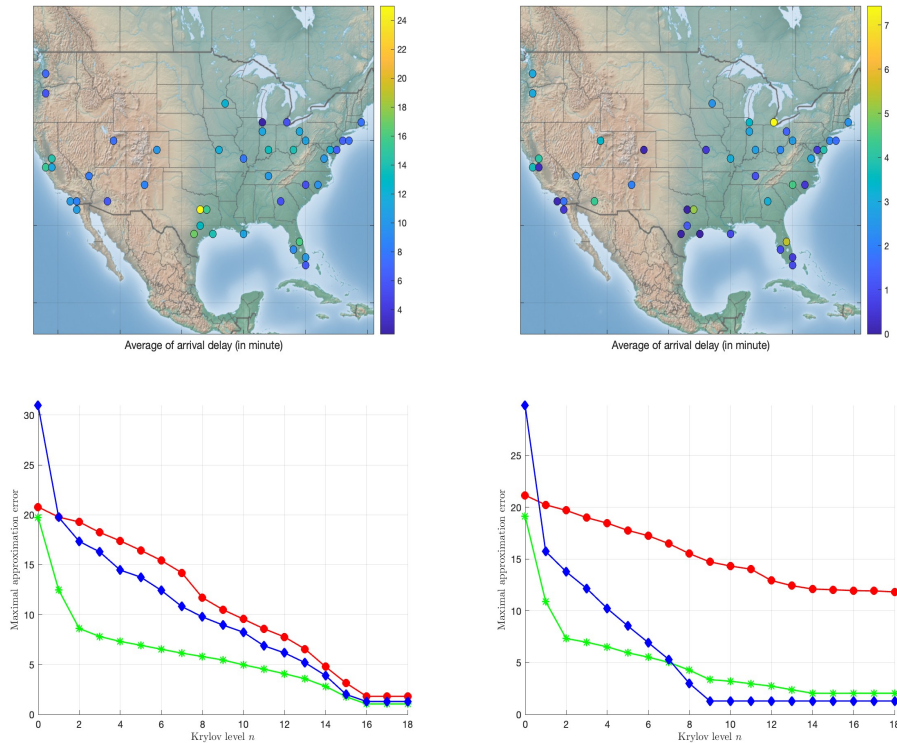


Fig. 2: Plotted on the top are the flight delay data \mathbf{x}_d (left) and absolute error data $|\mathbf{x}_{K;d,n} - \mathbf{x}_d|$ (right) of the top 50 US airports on 29 August 2024, except Honolulu International airport (HNL) and Luis Munoz Marin International airport (SJU), where $d = 60$, $\mathbf{x}_{K;d,n}$ is reconstructed from Algorithm V.1 in the noiseless environment with adaptive GSIS model and Krylov level $n = 2$, and maximal approximation error is $\|\mathbf{x}_{K;60,2} - \mathbf{x}_{60}\|_\infty = 7.9382$. Shown on the bottom are the average of maximal approximation error $F_{K,n}$ by Krylov subspaces of adaptive GSIS (in green) and of non-adaptive GSIS (in blue) and the maximal approximation error $F_{B,n}$ by bandlimited spaces (in red) over 184 days, where the subsampling set contains the whole 50 airports for the left plot and the top 30 airports with most delay on average over 184 days for the right plot.

over 184 days, where $\mathbf{x}_{K;d,n}$ is the signal in $H_{d,n}$ (respectively H_n) reconstructed from Algorithm V.1 in the noiseless environment with the identity matrix as the sampling matrix, and $\mathbf{x}_{B;d,n}$ is the projection of the graph signal \mathbf{x}_d on the bandlimiting space $B_{d,n}$ of lowest frequencies with its dimension being the same of the one of Krylov space, i.e., $\dim B_{d,n} = \dim H_{d,n}$. We also test the performance of Algorithm V.1 when the flight delay data on the 30 airports with top delay on average are available only, see the bottom right plot of Figure 2.

The measurements in (VI.4) can be used to measure the rationality to use GSISs and bandlimited spaces to model the flight delay dataset. From the plots on the top right and at the bottom of Figure 2, we see that the GSIS is more suitable to model flight delay dataset than the bandlimited space does, and that the GSIS with the generators chosen adaptively could further improve the performance. The reason could be that the flight delay data is more well-localized in spatial domain than concentrated on low frequency in the Fourier domain. In the United States, the words on time at the airport refer to any flight departure or flight arrival within less than 15 minutes of their scheduled time. We observe that the maximal Krylov approximation error with level $n = 2$ for the adaptive GSIS model is less than 9 minutes, which confirms the speculation that the flight delays at the US airport network are mostly caused by few airports and their subsequent ripple effect. For the scenario that only flight delay data on the top 30 airports with most delays is available, the corresponding data fitting via the nonadaptive/adaptive GSIS models have comparable performance, as we notice that the flight delay data at airports representing the supporting vertices of the generators in the nonadaptive GSIS are always available, while no airports with the most delays on some day, used for the adaptive GSIS, are included in those 30 airports with the most delays on average.

VII. PROOFS

In this section, we collect the proofs of Theorems III.1, III.2, IV.1 and IV.2.

A. Proof of Theorem III.1

The implications (iv) \implies (iii) \implies (ii) follow from the definition of a finite-generated shift-invariant space, and the implication (i) \implies (iv) holds by Theorem III.2 with its proof given in Appendix VII-B. Then it remains to prove the implication (ii) \implies (i).

For $1 \leq n \leq N$, let \mathbf{e}_n be the unit vector with zero entries except taking value one at n -th entries, and \mathbf{E}_n be the diagonal matrix with \mathbf{e}_n as the diagonal vector. By Assumption II.1, there exist polynomials $p_n, 1 \leq n \leq N$, of degree at most $N - 1$ such that

$$p_n(\mathbf{S}_1, \dots, \mathbf{S}_L) = \mathbf{U} \mathbf{E}_n \mathbf{U}^T, \quad 1 \leq n \leq N, \quad (\text{VII.1})$$

where \mathbf{U} is the orthogonal matrix in (II.2). In particular, the polynomials $p_n, 1 \leq n \leq N$, are chosen to satisfying the interpolation property

$$p_n(\mathbf{A}_m) = \delta_{nm}, \quad 1 \leq m, n \leq N, \quad (\text{VII.2})$$

where δ_{nm} is the standard Kronecker symbol [52].

For $1 \leq n \leq N$, let \mathbf{u}_n be the n -th column of the orthogonal matrix \mathbf{U} in (II.2), and set

$$G_n = p_n(\mathbf{S}_1, \dots, \mathbf{S}_L)H, \quad 1 \leq n \leq N. \quad (\text{VII.3})$$

Then one may verify that

$$G_n = \{\widehat{\mathbf{x}}(n)\mathbf{u}_n \mid \mathbf{x} \in H\}, \quad 1 \leq n \leq N, \quad (\text{VII.4})$$

where $\widehat{\mathbf{x}}(n) = \mathbf{e}_n^T \widehat{\mathbf{x}}$ is the n -th component of the Fourier transform $\widehat{\mathbf{x}}$ of a signal $\mathbf{x} \in H$. Therefore for any $1 \leq n \leq N$, either G_n is trivial or it has dimension one, i.e.,

$$\text{either } G_n = \{0\} \text{ or } G_n = \text{span } \mathbf{u}_n. \quad (\text{VII.5})$$

Let $\Omega = \{n \mid G_n \neq \{0\}\}$, and set

$$B_\Omega = \{\mathbf{x} \mid \text{supp } \widehat{\mathbf{x}} \subset \Omega\} = \bigoplus_{n \in \Omega} G_n. \quad (\text{VII.6})$$

By the shift-invariance assumption on H , we obtain from (VII.3) that $G_n \subset H, 1 \leq n \leq N$, and hence

$$B_\Omega \subset H \quad (\text{VII.7})$$

by (VII.5) and (VII.6). On the other hand, for any $\mathbf{x} \in H$, we obtained from (VII.3) and the definition of polynomials $p_n, 1 \leq n \leq N$, that

$$\mathbf{x} = \sum_{n=1}^N p_n(\mathbf{S}_1, \dots, \mathbf{S}_L)\mathbf{x} = \sum_{n \in \Omega} p_n(\mathbf{S}_1, \dots, \mathbf{S}_L)\mathbf{x} \in B_\Omega.$$

This together with (VII.7) proves that $H = B_\Omega$, and hence completes the proof of the implication (ii) \implies (i).

B. Proof of Theorem III.2

Let $\lambda(n), 1 \leq n \leq N$, be as in (II.3). By Assumption II.1, there exists a nonzero vector $\mathbf{d} = [d_1, \dots, d_L]^T \in \mathbb{R}^L$ such that $\mathbf{d}^T \lambda(n), 1 \leq n \leq N$, are distinct real numbers. Take $\mathbf{T} = \sum_{l=1}^L d_l \mathbf{S}_l$ and let ϕ_0 be as in (III.8). Then it remains to verify that

$$B_\Omega = \text{span}\{\mathbf{T}^m \phi_0, 0 \leq m \leq \#\Omega - 1\}. \quad (\text{VII.8})$$

By (II.6) and (III.8), we see that the Fourier transforms of $\mathbf{T}^m \phi_0, 0 \leq m \leq \#\Omega - 1$, are supported on Ω and hence

$$\text{span}\{\mathbf{T}^m \phi_0, 0 \leq m \leq \#\Omega - 1\} \subset B_\Omega. \quad (\text{VII.9})$$

Let $q_n, n \in \Omega$, be univariate polynomials of degree at most $\#\Omega - 1$ that satisfy the interpolation property

$$q_n(\mathbf{d}^T \lambda(n')) = \delta_{nn'}, \quad n, n' \in \Omega. \quad (\text{VII.10})$$

The existence of such a polynomial follows from the distinct assumption on $\mathbf{d}^T \boldsymbol{\lambda}(n')$, $n' \in \Omega$. By the construction of the graph shift \mathbf{T} , we see that $\mathbf{T} = \mathbf{U} \boldsymbol{\Lambda}_T \mathbf{U}^T$ for some diagonal matrix $\boldsymbol{\Lambda}_T$ with diagonal entries $\mathbf{d}^T \boldsymbol{\lambda}(n')$, $1 \leq n' \leq N$. Therefore

$$q_n(\mathbf{T}) = \mathbf{U} q_n(\boldsymbol{\Lambda}_T) \mathbf{U}^T \quad (\text{VII.11})$$

with the diagonal matrix $q_n(\boldsymbol{\Lambda}_T)$ having diagonal entries $q_n(\mathbf{d}^T \boldsymbol{\lambda}(n'))$, $1 \leq n' \leq N$.

Take arbitrary bandlimited signal $\mathbf{x} \in B_\Omega$. By (VII.10) and (VII.11), we have

$$\widehat{\mathbf{x}} = \sum_{n \in \Omega} \frac{\widehat{\mathbf{x}}(n)}{\widehat{\phi}_0(n)} q_n(\boldsymbol{\Lambda}_T) \widehat{\phi}_0.$$

Therefore taking the inverse Fourier transform \mathcal{F}^{-1} at both sides yields

$$\mathbf{x} = \sum_{n \in \Omega} \frac{\widehat{\mathbf{x}}(n)}{\widehat{\phi}_0(n)} q_n(\mathbf{T}) \phi_0.$$

This together with the degree property for the polynomials q_n , $n \in \Omega$ proves that

$$B_\Omega \subset \text{span}\{\mathbf{T}^m \phi_0, 0 \leq m \leq \#\Omega - 1\}. \quad (\text{VII.12})$$

Combining (VII.9) and (VII.12) proves (VII.8) and hence completes the proof of Theorem III.2.

C. Proof of Theorem IV.1

By Theorem III.1, there exists $\Omega \subset \{1, \dots, N\}$ such that (III.2) holds. Define the kernel \mathbf{K} by

$$\mathbf{K} = \mathbf{U} \boldsymbol{\Lambda}_\Omega \mathbf{U}^T, \quad (\text{VII.13})$$

where \mathbf{U} is the orthogonal matrix in (II.2) and $\boldsymbol{\Lambda}_\Omega$ is the diagonal matrix in (IV.3). Then we obtain from (II.2) and (VII.13) that the kernel \mathbf{K} in (VII.13) is shift-invariant.

Let $\boldsymbol{\delta}_j$, $j \in V$, be delta signals taking value zero at all vertices except value one at the vertex j . By (III.2) and (VII.13), the linear space H is spanned by $\mathbf{K} \boldsymbol{\delta}_j$, $j \in V$, and satisfies the following reproducing kernel property,

$$\mathbf{x} = \mathbf{K} \mathbf{x}, \quad \mathbf{x} \in H,$$

where the standard Euclidean inner product on \mathbb{R}^N is used for its linear subspace $H \subset \mathbb{R}^N$. This completes the proof that H is a reproducing kernel space with the shift-invariant space \mathbf{K} .

D. Proof of Theorem IV.2

Let \mathbf{K} be the shift-invariant kernel of the RKHS H , and let \mathbf{x}, \mathbf{y} be two arbitrary elements in H . By (IV.2) and the definition of the inner product on the RKHS H ,

$$\langle \mathbf{x}, \mathbf{y} \rangle_H = \mathbf{c}^T \mathbf{K} \mathbf{d}. \quad (\text{VII.14})$$

for some \mathbf{c} and $\mathbf{d} \in \mathbb{R}^N$ with $\mathbf{x} = \mathbf{K} \mathbf{c}$ and $\mathbf{y} = \mathbf{K} \mathbf{d}$.

By Theorem A.3 in [34] and Assumption II.1, there exists a diagonal matrix $\boldsymbol{\Lambda}$ for the shift-invariant kernel \mathbf{K} such that $\mathbf{K} = \mathbf{U} \boldsymbol{\Lambda} \mathbf{U}^T$, where \mathbf{U} is the orthogonal matrix in (II.2). Denote the pseudo-inverse of the diagonal matrix $\boldsymbol{\Lambda}$ by $\boldsymbol{\Lambda}^\dagger$. Then it follows from (VII.14) that $\widehat{\mathbf{x}} = \boldsymbol{\Lambda} \widehat{\mathbf{c}}$, $\widehat{\mathbf{y}} = \boldsymbol{\Lambda} \widehat{\mathbf{d}}$ and

$$\langle \mathbf{x}, \mathbf{y} \rangle_H = \widehat{\mathbf{c}}^T \boldsymbol{\Lambda} \widehat{\mathbf{d}} = \widehat{\mathbf{c}}^T \boldsymbol{\Lambda} \boldsymbol{\Lambda}^\dagger \boldsymbol{\Lambda} \widehat{\mathbf{d}} = \widehat{\mathbf{x}}^T \boldsymbol{\Lambda}^\dagger \widehat{\mathbf{y}}.$$

As \mathbf{K} is a reproducing kernel, it is represented by a positive semidefinite matrix, which implies that $\boldsymbol{\Lambda}^\dagger$ has nonnegative entries. Therefore (IV.4) holds and the proof is completed.

REFERENCES

- [1] I. Daubechies, *Ten Lectures on Wavelets*, SIAM, Philadelphia, 1992.
- [2] S. Mallat, *A Wavelet Tour of Signal Processing*, Academic Press, San Diego, CA, 1998.
- [3] M. Unser, “Sampling-50 years after Shannon,” *Proc. IEEE*, vol. 88, no. 4, pp. 569–587, 2000.
- [4] K. Grochenig, *Foundations of Time-Frequency Analysis*, Birkhauser, Boston, 2001.
- [5] A. Aldroubi and K. Grochenig, “Nonuniform sampling and reconstruction in shift-invariant spaces,” *SIAM Review*, vol. 43, no. 4, pp. 585–620, 2001.
- [6] A. Aldroubi, Q. Sun, and W. S. Tang, “ p -frames and shift invariant spaces of L_p ,” *J. Fourier Anal. Appl.*, vol. 7, pp. 1–21, 2001.
- [7] A. Aldroubi, Q. Sun, and W.-S. Tang, “Convolution, average sampling, and a Calderon resolution of the identity for shift-invariant spaces,” *J. Fourier Anal. Appl.*, vol. 11, pp. 215–244, 2005.
- [8] D. I. Shuman, S. K. Narang, P. Frossard, A. Ortega, and P. Vandergheynst, “The emerging field of signal processing on graphs: Extending high-dimensional data analysis to networks and other irregular domains,” *IEEE Signal Process. Mag.*, vol. 30, pp. 83–98, 2013.
- [9] A. Ortega, P. Frossard, Kovacevic, J. M. F. Moura, and P. Vandergheynst, “Graph signal processing: Overview, challenges, and applications,” *Proc. IEEE*, vol. 106, no. 5, pp. 808–828, 2018.
- [10] L. Stankovic, M. Dakovic, and E. Sejdic, “Introduction to Graph Signal Processing,” *Vertex-Frequency Analysis of Graph Signals*, Springer Cham, pp. 3–108, 2019.
- [11] X. Dong, D. Thanou, L. Toni, M. Bronstein, and P. Frossard, “Graph signal processing for machine learning: A review and new perspectives,” *IEEE Signal Process. Mag.*, vol. 37, pp. 117–127, 2020.
- [12] A. Ortega, *Introduction to Graph Signal Processing*, Cambridge University Press, 2022.
- [13] E. Isufi, F. Gama, D. I. Shuman, and S. Segarra, “Graph filters for signal processing and machine learning on graphs,” *IEEE Trans. Signal Process.*, 32 pp., 2024, DOI: 10.1109/TSP.2024.3349788
- [14] I. Pesenson, “Sampling in Paley-Wiener spaces on combinatorial graphs,” *Trans. Amer. Math. Soc.*, vol. 360, no. 10, pp. 5603–5627, 2008.
- [15] I. Pesenson, “Variational splines and Paley-Wiener spaces on combinatorial graphs,” *Constr. Approx.*, vol. 29, no. 1, pp. 1–21, 2009.
- [16] S. Chen, R. Varma, A. Sandryhaila, and J. Kovaevi, “Discrete signal processing on graphs: sampling theory,” *IEEE Trans. Signal Process.*, vol. 63, no. 24, pp. 6510–6523, 2015.
- [17] A. Anis, A. Gadde, and A. Ortega, “Efficient sampling set selection for bandlimited graph signals using graph spectral proxies,” *IEEE Trans. Signal Process.*, vol. 64, no. 14, pp. 3775–3789, 2016.
- [18] G. Puy, N. Tremblay, R. Gribonval, and P. Vandergheynst, “Random sampling of bandlimited signals on graphs,” *Appl. Comput. Harmon. Anal.*, vol. 44, no. 2, pp. 446–475, 2018.
- [19] C. Huang, Q. Zhang, J. Huang, and L. Yang, “Reconstruction of bandlimited graph signals from measurements,” *Digit. Signal Process.*, vol. 101, article no. 102728, 13 pp., 2020.
- [20] B. Scholkopf and A. J. Smola, *Learning with Kernels: Support Vector Machines, Regularization, Optimization, and Beyond*, MIT Press, Cambridge, Massachusetts, 2002.
- [21] H. Zhang, Y. Xu, and J. Zhang, “Reproducing kernel Banach spaces for machine learning,” *J. Mach. Learn. Res.*, vol. 10, pp. 2741–2775, 2009.
- [22] S. Shalev-Shwartz and S. Ben-David, *Understanding Machine Learning: From Theory to Algorithms*, Cambridge University Press, 2014.
- [23] G. Nikolentzos, G. Siglidis, and M. Vazirgiannis, “Graph kernels: a survey,” *J. Artif. Intell. Res.*, vol. 72, pp. 943–1027, 2021.
- [24] S. Y. Chung and Q. Sun, “Barron space for graph convolution neural networks,” *arXiv preprint arXiv:2311.02838*, 37 pp., 2023.
- [25] R. S. Kondor and J. Lafferty, “Diffusion kernels on graphs and other discrete structures,” *Proc. ICML*, vol. 2, 8 pp. 2002.
- [26] A. J. Smola and R. Kondor, “Kernels and regularization on graphs,” *Learning Theory and Kernel Machines*, Lecture Notes in Computer Science, vol. 2777, Springer, Berlin, Heidelberg, 15 pp., 2003.
- [27] D. Zhou and B. Scholkopf, “A regularization framework for learning from graph data,” *Proc. ICML Workshop Statist. Relational Learn. Connections Other Fields*, Banff, Canada, Jul. 2004, vol. 15, pp. 67–68.
- [28] M. Belkin, P. Niyogi, and V. Sindhwani, “Manifold regularization: a geometric framework for learning from labeled and unlabeled examples,” *J. Mach. Learn. Res.*, vol. 7, pp. 2399–2434, 2006.
- [29] M. Seto, S. Suda, and T. Taniguchic, “Gram matrices of reproducing kernel Hilbert spaces over graphs,” *Linear Algebra Appl.*, volume 445, pp. 56–68, 2014.
- [30] P. A. Forero, K. Rajawat, and G. B. Giannakis, “Prediction of partially observed dynamical processes over networks via dictionary learning,” *IEEE Trans. Signal Process.*, vol. 62, no. 13, pp. 3305–3320, 2014.
- [31] M. S. Kotzagiannidis and P. L. Dragotti, “Sampling and reconstruction of sparse signals on circulant graphs — an introduction to graph-FRI,” *Appl. Comput. Harmon. Anal.*, vol. 47, no. 3, pp. 539–565, 2019.
- [32] D. Romero, M. Ma, and G. B. Giannakis, “Kernel-based reconstruction of graph signals,” *IEEE Trans. Signal Process.*, vol. 65, no. 3, pp. 764–778, 2017.
- [33] J. P. Ward, F. J. Narcowich, and J. D. Ward, “Interpolating splines on graphs for data science applications,” *Appl. Comput. Harmon. Anal.*, vol. 49, no. 2, pp. 540–557, 2020.
- [34] N. Emirov, C. Cheng, J. Jiang, and Q. Sun, “Polynomial graph filters of multiple shifts and distributed implementation of inverse filtering,” *Sampl. Theory Signal Process. Data Anal.*, vol. 20, article no. 2, 2022.
- [35] X. Jian and W. P. Tay, “Kernel ridge regression for generalized graph signal processing,” *2023 IEEE International Conference on Acoustics, Speech and Signal Processing (ICASSP)*, Rhodes Island, Greece, June 2023, pp. 1–5.
- [36] M. Z. Nashed and Q. Sun, “Sampling and reconstruction of signals in a reproducing kernel subspace of $L^p(\mathbb{R}^d)$,” *J. Funct. Anal.*, vol. 258, pp. 2422–2452, 2010.

- [37] A. Sandryhaila, and J. M. F. Moura, “Discrete signal processing on graphs,” *IEEE Trans. Signal Process.*, vol. 61, pp. 1644–1656, 2013.
- [38] A. Sandryhaila, and J. M. F. Moura, “Discrete signal processing on graphs: Frequency analysis,” *IEEE Trans. Signal Process.*, vol. 62, pp. 3042–3054, 2014.
- [39] J. Jiang, C. Cheng and Q. Sun, “Nonsubsampled graph filter banks: theory and distributed algorithms,” *IEEE Trans. Signal Process.*, vol. 67, pp. 3938–3953, 2019.
- [40] F. R. K. Chung, *Spectral Graph Theory*, CBMS Regional Conference Series in Mathematics, No. 92. Providence, RI, Amer. Math. Soc., 1997.
- [41] B. Ricaud, P. Borgnat, N. Tremblay, P. Goncalves, and P. Vandergheynst, “Fourier could be a data scientist: from graph Fourier transform to signal processing on graphs,” *C. R. Phys.*, vol. 20, pp. 474–488, 2019.
- [42] Y. Chen, C. Cheng, and Q. Sun, “Graph Fourier transform based on singular value decomposition of directed Laplacian,” *Sampl. Theory Signal Process. Data Anal.*, vol. 21, article no. 24, 28 pp., 2023.
- [43] C. Cheng, Y. Chen, Y. J. Lee, and Q. Sun, “SVD-based graph Fourier transforms on directed product graphs,” *IEEE Trans. Signal Inf. Process. Netw.*, vol. 9, pp. 531–541, 2023.
- [44] E. Rebrova, and P. Salanevich, “On graph uncertainty principle and eigenvector delocalization,” *arXiv preprint arXiv:2306.15810*, 13 pp., 2023.
- [45] D. L. Donoho and P. B. Stark, “Uncertainty principles and signal recovery,” *SIAM J. Math. Anal.*, vol. 49, no. 3, pp. 906–931, 1989.
- [46] O. Teke and P. P. Vaidyanathan. “Uncertainty principles and sparse eigenvectors of graphs,” *IEEE Trans. Signal Process.*, vol. 65, no. 20, pp. 5406–5420, 2017.
- [47] A. Aldroubi, J. Davis, and I. Krishtal, “Dynamical sampling: Time–space trade-off,” *Appl. Comput. Harmon. Anal.*, vol. 34, no. 3, pp. 495–503, 2013.
- [48] A. G. Marques, S. Segarra, G. Leus, and A. Ribeiro, “Sampling of graph signals with successive local aggregations,” *IEEE Trans. Signal Process.*, vol. 64, no. 7, pp. 1832–1843, 2016.
- [49] A. Aldroubi, C. Cabrelli, U. Molter, and S. Tang, “Dynamical sampling,” *Appl. Comput. Harmon. Anal.*, vol. 42, no. 3, pp. 378–401, 2017.
- [50] L. Huang, D. Needell, and S. Tang, “Robust recovery of bandlimited graph signals via randomized dynamical sampling,” *arXiv preprint arXiv:2109.14079*, 34 pp., 2021.
- [51] Airline On-Time Performance Data collected by Bureau of Transportation Statistics, <http://www.transtats.bts.gov/>
- [52] E. W. Cheney and W. A. Light, *A Course in Approximation Theory*, Graduate Studies in Mathematics 101, Amer. Math. Soc., 2000.